Assessment of risk of freeze-thaw damage in internally insulated masonry in a changing climate

Xiaohai Zhou[1, 2], **Jan Carmeliet**[2] **and Dominique Derome**[3]

[1]Laboratory of Multiscale Studies in Building Physics, Empa, Dübendorf, Switzerland

[2]Chair of Building Physics, ETH Zürich, Zürich, Switzerland

[3]Assessment of risk of freeze-thaw damage in internally insulated masonry in a changing climate

Abstract

Buildings are susceptible to gradual changes in climate and to extreme events. The scale and severity of climate change are expected to be spatially heterogeneous. There is a necessity to consider changing climate in the operation and maintenance of buildings, as buildings have a long-term service life. In this study, the impact of climate change on the risk of freeze-thaw damage for internally insulated masonry wall in two regions in Switzerland (Zurich and Davos) for two future periods is investigated. A hygrothermal model that considers coupled moisture and heat transport in freezing and non-freezing building materials is used. The risk of freeze-thaw damage is evaluated with an indicator, called the FTDR Index. Climate projections under A1B and A2 emission scenarios from ten different climate model chains are chosen to cover a wide range of possible future climates. The risk of freeze-thaw damage at Zurich is relatively high in the reference period. An increase in air temperature in the cold period that leads to less freeze-thaw cycles is the main reason for the lower risk of freeze-thaw damage in the future periods. By comparison, the risk of freeze-thaw damage at Davos is low in the reference period. An increase in temperature and precipitation in the cold period is the main reason for the higher risk of freeze-thaw damage in the future periods at Davos. In the face of climate change, the future requirement on frost resistance of building materials and components at Davos should take the future climate loading into account.

Keywords: hygrothermal modeling; freeze-thaw damage; climate change; internal thermal insulation

1 Introduction

Climate change in the world is now known to be very likely caused by anthropogenic greenhouse gas emissions, however the future evolution and its impacts are still uncertain. Different emission scenarios for climate change have been proposed by the Intergovernmental Panel on Climate Change (IPCC). The global average surface temperature in 2090-2099 will likely be 1.7-4.4 degrees higher than in 1980-1999 according

to its A1B emission scenario whereas it will likely be 2.0-5.4 degrees higher according to the A2 emission scenario [1]. The A1B emission scenario describes a future world of very rapid economic growth with a balance across all energy sources while the A2 emission scenario describes a very heterogeneous world with self-reliant nations and fragmented economic development [2]. For Switzerland, it is projected that there will be an increase of seasonal mean temperature of 2.7–4.1 degrees for the A1B scenario and 3.2–4.8 degrees for the A2 scenario from 2070–2099 compared to the reference period 1980-2009. Summer mean precipitation will likely decrease all over Switzerland, while winter precipitation will likely increase in Switzerland. The scale and severity of climate change are expected to be spatially heterogeneous and the socio-economic impacts they cause can vary regionally. High latitude and mountainous regions are among the most affected and vulnerable areas. Switzerland is particularly affected by climate change, as temperatures here rise twice as fast as the global average [3]. In recognition of the anthropogenic cause of climate change, the Swiss government will halve its greenhouse gas emissions by 2030 compared with 1990 levels and reduce its net carbon emissions to zero by 2050 [4]. This climate target ensures that Switzerland will make its contribution to limiting global warming to less than 1.5 degrees.

Building performance will be affected either by the gradual changes in climate such as increased levels of precipitation or increased temperature or by the increase frequency of extreme weather events. A substantial of studies on the impact of climate change on buildings focused on the impact on energy use for heating and cooling [6]. The number of studies on the impact of future climate on the durability and hygrothermal performance of buildings is limited. Lacasse [7] presented an overview of durability and climate change of building materials, components, and assemblies. There is a necessity to consider changing climate in the operation and maintenance of buildings, as buildings have a long-term service life. Building codes need to be developed which consider future climate design [8]. The challenges of using future climate data in the hygrothermal simulation of buildings have been discussed in [9–12]. Moisture play a crucial role in building durability, performance, comfort and efficiency. Moisture-related damage problems in buildings are erosion and corrosion of building materials, salt crystallization, freeze-thaw damage and mould growth etc. Building damage caused by moisture can be exceptionally expensive. The EU Project Noah's Ark presented that the main climate changes threatening cultural heritage are rising temperatures, enhanced amounts of precipitation and sea level rise [13]. Higher amount of precipitation will lead to higher moisture damage risk by increasing exterior moisture load and indoor relative humidity. Many buildings are vulnerable to higher moisture risk under climate change. Building facades of Finnish concrete buildings will receive more wind-driving rain load in the future because of increased precipitation [14]. A study of the impact

of climate change on wind-driven rain for building facades in Gothenburg, Sweden indicates that higher amounts of moisture will accumulate in walls in the future [10]. For two historic museum buildings in Netherlands and Belgium, the projected climate change increases considerably indoor relative humidity and leads to increased risk of mould growth [15]. The risk of mould growth in attics in Sweden tends to increase considering climate change scenarios [9,16,17]. Mould growth risk in retrofitted double-stud assembly in Montreal, Canada under future climatic conditions will increase considerably [18].

Compared to common moisture-related problems in buildings, freeze-thaw damage of building materials can be affected by both changes in temperature and precipitation. It becomes even more complicated as air temperature change has an influence on the form of precipitation. When the atmospheric temperature is above 0 °C, freezing does not occur and no ice exists in building materials. When the atmospheric temperature is at or below freezing (0 °C), precipitation will be in the form of snow, resulting in no wind-driven rain load to the building surface and consequently no water uptake in building materials. The risk of freeze-thaw damage in building materials under climate change will be quite different in different regions. For regions with temperate climates, the risk of freeze-thaw damage is likely to decrease under climate change [19–21]. However, for high-altitude and high-latitude regions, an increase in the risk of freeze-thaw damage is highly likely under climate change [22–24]. For example, the risk of freeze-thaw damage of concrete facades and balconies in the southern coastal area of Finland will decrease due to increase of air temperature whereas the risk will increase in the inland areas due to the increasing amount of rain [24]. Temperate Europe will have smaller freeze-thaw damage risk on built heritage and archaeological sites due to increase of air temperature under climate change [20]. The double effect of climate change and urban heat island effect will significantly lower the risk of freeze–thaw damage in the urban central area of Ghent, Belgium [21].

The mechanism responsible for freeze-thaw damage in porous building materials is the pressure that the ice crystal growth generates on the internal solid walls of the porous solid [25]. The crystal pressure leads to a tensile stress within the surrounding solid matrix. Damage occurs when the tensile stress is larger than the strength of solid matrix [26]. Water in porous building materials freezes at temperatures below 0 °C, varying in the function of the pore size, the smaller the pore, the lower the freezing temperature [27,28]. It has been shown that freeze-thaw cycle does not necessarily lead to damage in porous building materials and the most critical factor for the occurrence of freeze-thaw damage is the level of moisture content (degree of saturation) at the time of freezing in porous building materials [29–31].

Internal thermal insulation is the main retrofit solution for historical buildings with a worth-

preserving façade to improve building energy efficiency [32–35]. However, the addition of insulation to the inside of existing walls may significantly increase the risk of freeze-thaw damage due to increased moisture levels and decreased temperature in the walls, often load-bearing clay brick or stone masonry. For example, Maurenbrecher et al. found that temperature in the masonry of an internally insulated 765-mm thick masonry wall drops below freezing temperature for several months in the winter [36]. Künzel found more than 50% increase of annual mean moisture content in some parts of the masonry after the addition of internal thermal insulation [37]. Zhou et al. found that ice content in the masonry wall can increase significantly after the addition of internal thermal insulation [38]. Therefore, it is essential to assess the risks of freeze-thaw damage for internally insulated building envelopes under different climate change scenarios so that adaptation and mitigation measures can be made to reduce the effects in terms of social and economic losses.

Evaluation of climate change impacts needs to consider uncertainties in future climate. Three categories of uncertainties can be derived from climate change projections: (i) emission scenario uncertainty, (ii) climate model uncertainty, and (iii) natural variability. Emission scenario uncertainty reflects the uncertainty in global socio-economic development and associated greenhouse gas emissions. Climate model uncertainties include uncertainties associated with limited understanding of physical processes in the global climate system and the difficulties of representing them in climate models [39,40]. Observational uncertainty in evaluation data and parameterizations, choice of model domain and application of boundary conditions all affect the accuracy of climate models. Natural internal variability is the interannual to decadal variability caused by coupled ocean-atmosphere interaction such as the El Niño Southern Oscillation or the North Atlantic Oscillation. Climate change uncertainties can be evaluated by utilization of projections from an ensemble of different climate models under different emission scenarios.

The objective of this study is to assess the risk of freeze-thaw damage of internally insulated masonry under climate change in Switzerland. Two locations with very different climatic conditions are selected for analysis. The studied wall envelope is a masonry wall internally insulated with vapor-open, non-capillary active insulation material. A hygrothermal model that takes into account the coupled moisture and heat transport in porous building materials and tracks the occurrence of freezing and thawing in function of pore size distribution is used. Hygrothermal simulations are performed to predict temperature and ice content distribution in the wall envelopes and the risk of freeze-thaw damage is evaluated based on a hygrothermal performance indicator. The influence of future periods, emission scenarios and climate models on the risk of freeze-thaw damage at the two locations is examined.

2 Methodology

2.1 Study locations

The study investigates two locations in Switzerland: Zurich and Davos. The two locations have very different climatic conditions. Zurich is located to the north of the Alps at an elevation of 408 m above sea level. The climate is characterized by mild winter and warm summer. In Zurich, the annual mean temperature is 9.3 °C and the annual precipitation is 1101 mm. By comparison, Davos is located in the Alps at an elevation of 1506 m above sea level. It has a cold climate with an annual mean temperature of 3.9 °C. It receives about 1000 mm of precipitation annually. The average daily temperature and five-day accumulated precipitation at Zurich and Davos averaged over a period from 1981 to 2010 are shown in Figure 1. In winter, the average daily temperature from 1981-2010 at Zurich is slightly above 0.0 °C whereas it is much lower than 0.0 °C at Davos. Precipitation mainly occurs in the form of rain in winter at Zurich due to low high temperature, whereas precipitation mainly occurs in the form of snow in winter at Davos due to low air temperature.

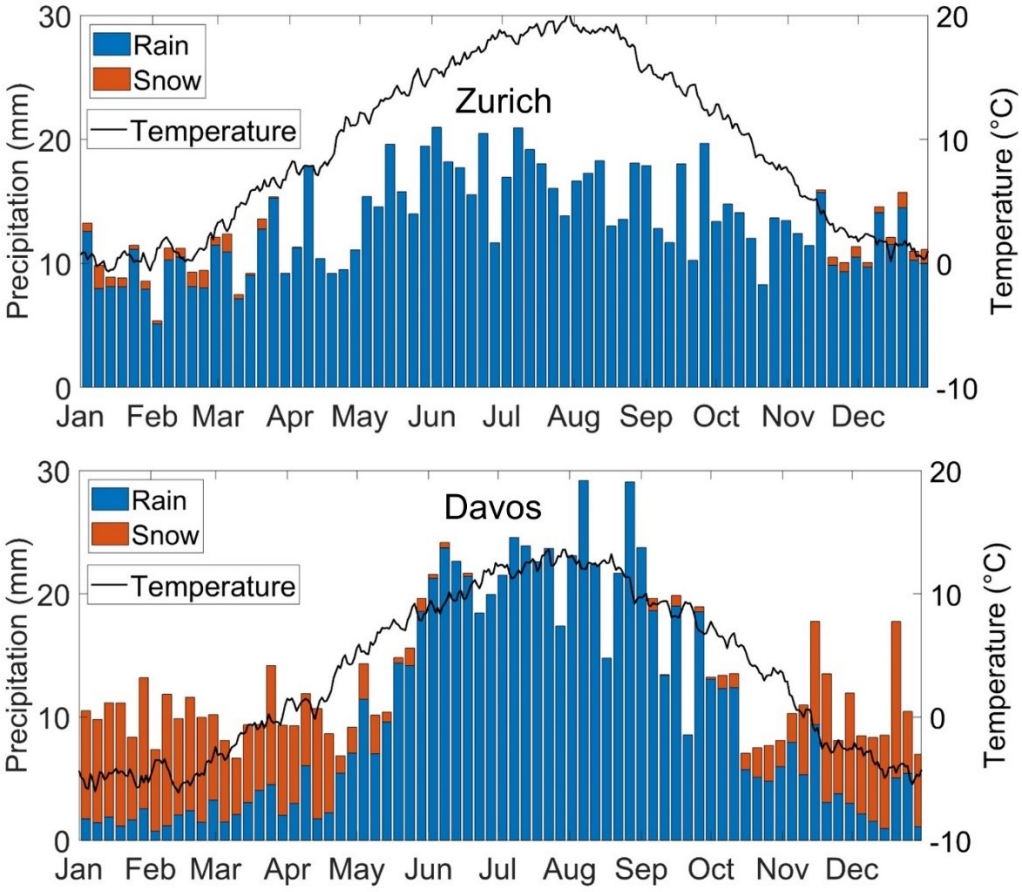

Figure 1. Average daily temperature and five-day accumulated rain and snow in Zurich and Davos averaged over the period from 1981 to 2010

2.2 Wall materials and envelopes

Masonry is the most common wall structure for buildings in Switzerland. Internally insulated masonry walls present much higher risk of freeze-thaw damage than non-insulated and externally insulated masonry walls. Therefore, an internally insulated masonry wall is selected for analysis. The internally insulated masonry wall consists starting from the outside of a three-wythe masonry assembly, a layer of plaster on the original wall, an added layer of insulating plaster, which is of the vapor-open non capillary active type, and an added layer of finishing plaster. The material properties of clay brick, cement mortar and insulation plaster are from Guizzardi [41] while the material properties of plaster are from the HAMFEM database [42]. The wall orientation with the largest wind-driven rain load is selected for analysis, which is 240 degree from north for Zurich (SSW) and 30 degree for Davos (NNE) [32].

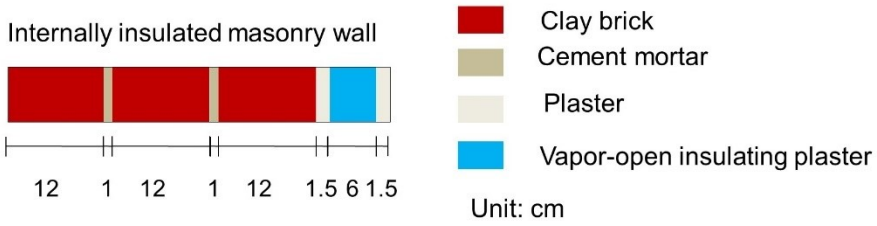

Figure 2. Masonry wall envelope

2.3 Future climate scenarios and meteorological data

The climate change scenarios are from the Swiss Climate Change Scenarios CH2011 [39,43]. The Swiss Climate Change Scenarios CH2011 contains data for all stations of the MeteoSwiss monitoring networks for the future periods of 2021-2050 and 2070-2099. The data are daily additive temperature changes and daily multiplicative precipitation changes to the reference period 1980-2009 from ten different GCM-RCM model chains. Two scenarios of emission projections are available for future climate: the A1B and A2 emissions scenarios. The daily variations of temperature and precipitation for Zurich and Davos for the future periods of 2021-2050 and 2070-2099 under different emission scenarios are shown in Figures 3 and 4. For freeze-thaw damage problems, change of temperature and precipitation in the cold period of the year can have a very large influence. Therefore, changes in average temperature and precipitation in the cold period from November to March are selected for analysis (Figure 5). All climate scenarios show increased temperature in the cold period in future for both Zurich and Davos compared to

the reference period (Figure 5). The increase of temperature for the 2021-2050 period is larger for the A1B scenarios than A2 scenarios at Zurich and Davos, whereas the increase of temperature for the 2070-2099 period is larger for the A2 scenarios than A1B scenarios. For example, for the 2021-2050 period at Davos, there is a mean temperature increase of 0.66–1.67 K for the A1B scenario and 0.66–1.45 K for the A2 scenario. For the 2070-2099 period at Davos, there is a mean temperature increase of 2.00–3.54 K for the A1B scenario and 2.43–4.17 K for the A2 scenario. Mean temperature change in the cold period at Zurich is smaller than that in Davos. For the 2021-2050 period at Zurich, there is a mean temperature increase of 0.66–1.62 K. For the 2070-2099, there is a mean temperature increase of 1.94–3.76 K. Among all the climate model chains, the chain HadCM3Q0_HadCM3Q0 (HH) shows almost the largest cold period temperature increase whereas the chain BCM_RCA (BR) shows the lowest temperature increase (Figure 5).

In future, most projections indicate increased mean annual precipitation for Zurich and Davos. For most projections, summer precipitation is expected to decrease whereas winter precipitation is expected to increase (Figures 3 and 4). Precipitation change in the cold time in the 2021-2050 period is much smaller than that in the 2070-2099 period (Figure 5). For the 2021-2050 period at Zurich, the change of cold period precipitation is -2.0 to 18.6 % for the A1B scenario and -1.5 to 16.8 % for the A2 scenario. For the 2070-2099 period, the change of winter precipitation is -4.1 to 25.5 % for the A1B scenario and -4.8 to 29.0 % for the A2 scenario. The climate model chains that has larger precipitation change in the period 2021-2050 presents also larger precipitation change in the period 2070-2099. For the 2021-2050 period at Davos, the change of cold period precipitation is -4.5 to 9.9 % for the A1B scenario and -3.6 to 8.8% for the A2 scenario (Figure 5). For the 2070-2099 period, the change of cold period precipitation is -12.1 to 20.9 % for the A1B scenario and -14.3 to 23.4 % for the A2 scenario. The climate model chains that has larger precipitation change in the period 2021-2050 do not necessarily have larger precipitation change in the period 2070-2099 at Davos.

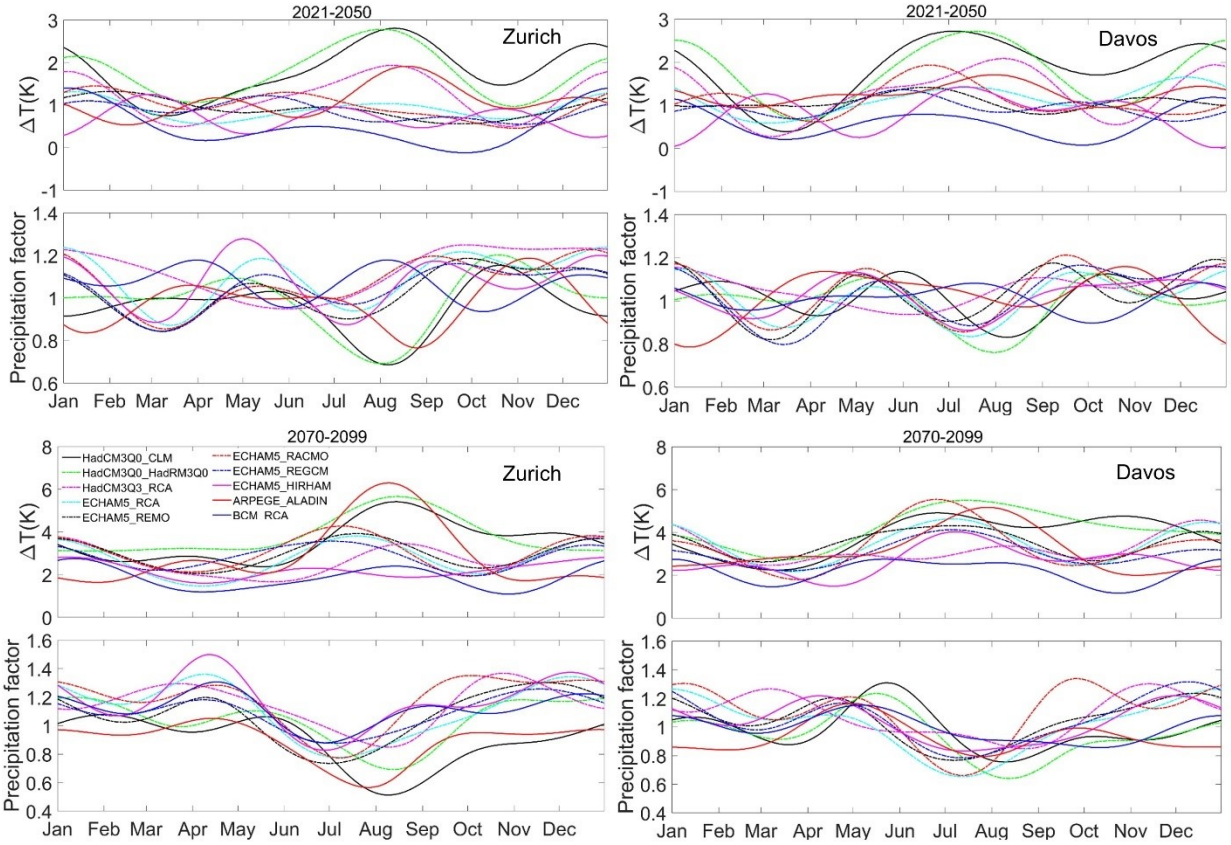

Figure 3. Future climate scenarios for the 2010-2050 and 2070-2099 periods at Zurich and Davos for A1B scenario for the ten GCM-RCM model chains.

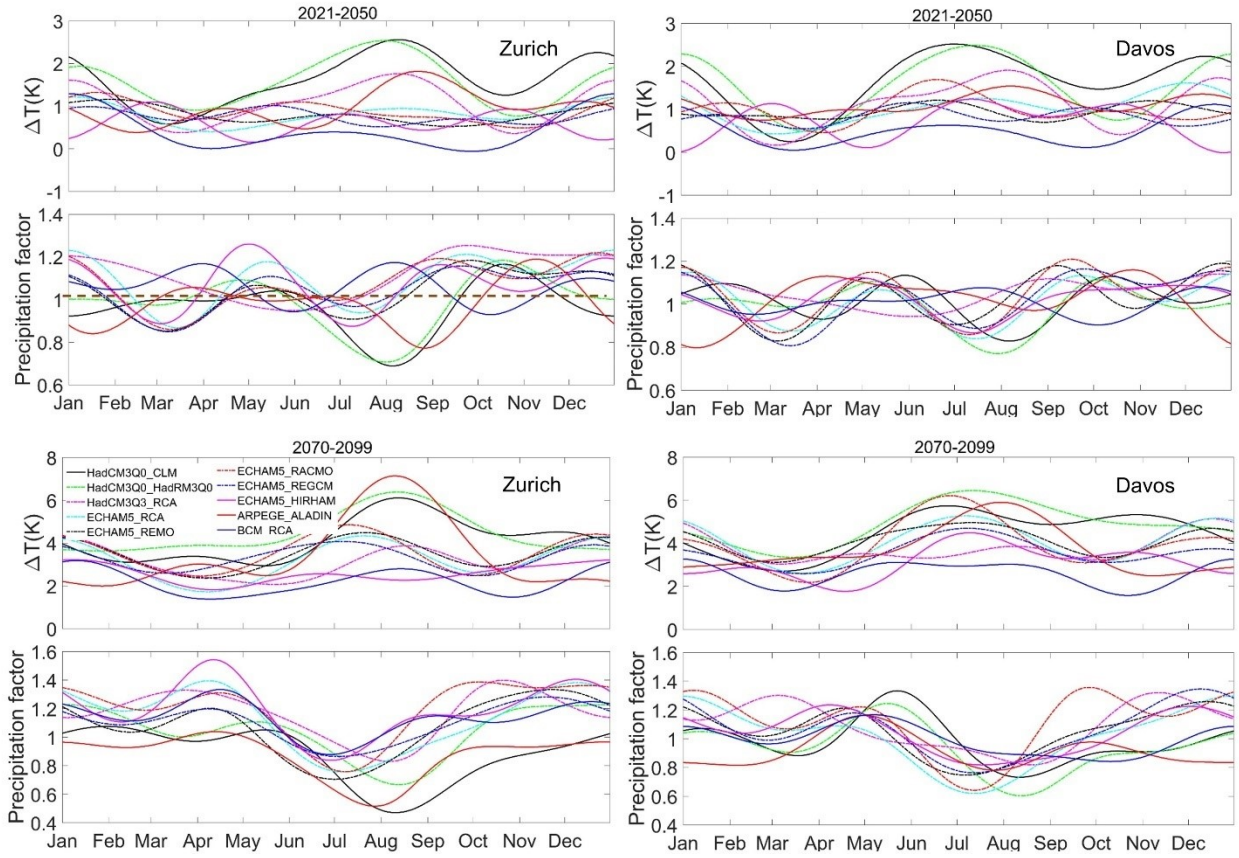

Figure 4. Future climate scenarios for the 2021-2050 and 2070-2099 periods at Zurich and Davos for A2 scenario for the ten GCM-RCM model chains.

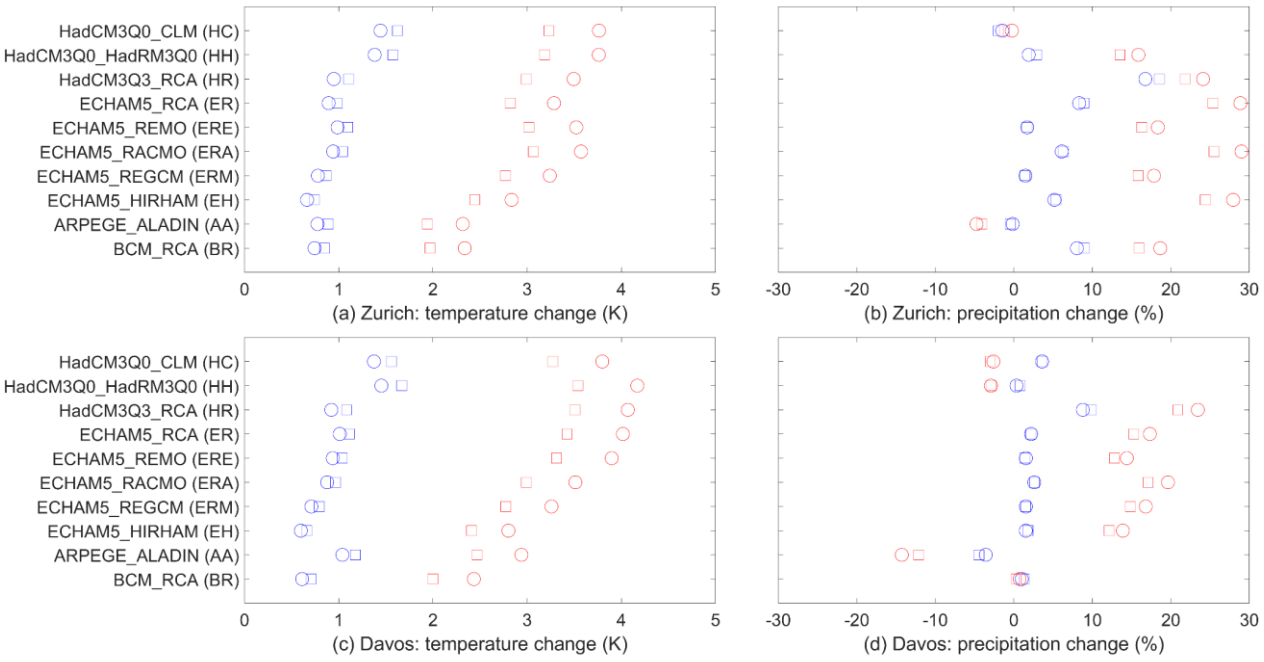

Figure 5. Change in average temperature and precipitation from November to March for Zurich and Davos for the ten GCM-RCM model chains compared to the reference period 1980-2009. Scenarios are A1B (square) and A2 (Circle), 2021-2050 period (blue) and 2070-2099 period (red).

The reference simulation period covers the time period 1981-2010, due to unavailability of meteorological data in 1980. The following hourly meteorological data are used for the analysis: air temperature, precipitation, relative humidity, wind velocity and direction and global radiation. When the air temperature is above 0.0 °C, the precipitation is in the form of rain and when the air temperature is at or below 0.0 °C, the precipitation is in the form of snow. The hourly meteorological data are from MeteoSwiss monitoring stations of Zurich Kloten and Davos. The future climate scenarios for the period 2021-2050 and 2070-2099 are simulated with the same data of the period 1981-2010 modified by the respective changes of additive temperature and multiplicative precipitation.

The wind-driven rain load for wall envelope is calculated according to ASHRAE Standard 160 - Criteria for Moisture Control Design Analysis in Buildings [44], where the WDR intensity (R_{WDR}) is defined by the following equation:

$$R_{WDR} = R_h \times F_E \times F_D \times 0.2 \times V_{10} \times \cos\theta \quad (1)$$

where R_h is the horizontal rainfall amount (kg $m^{-2}h^{-1}$ or mm h^{-1}); F_E is the rain exposure factor; F_D is the rain deposition factor; V_{10} is the wind speed at 10 m above ground (ms^{-1});

θ is the angle between the wind direction and the normal to the façade (rad). Factor F_E depends on the surrounding terrain and the height of the building, while Factor F_D describes the influence of the building itself. It is important to note that in a changing climate we only consider the change in horizontal rainfall amount, since information on changes in wind speed and wind direction are not available for Switzerland.

2.4 Hygrothermal model

The hygrothermal model developed by Zhou et al. [38] is used in this study. The model has been verified and validated by laboratory hygrothermal experiments. The hygrothermal model takes into account the coupled moisture and heat transport in porous medium and tracks the occurrence of freezing and thawing in function of pore size distribution and as well as ice content. The amount of ice content is equal to the difference between total moisture content and unfrozen liquid content. When there is no freezing, the difference between total moisture content and unfrozen liquid content becomes 0. Freezing and melting of water in porous medium is implemented based on the theory of freezing point depression, as freezing temperature of water in porous medium depends on pore size, i.e. water in the smaller pores freezes at temperatures lower than 0° C. An important function of the hygrothermal model is that it simulates also freezing-induced moisture migration. During freezing, due to the movement of moisture from unfrozen to freezing zones, the total moisture content and the ice content increase in the freezing zones [45].

2.5 Risk of freeze-thaw damage

The risk of freeze-thaw damage (FTDR) is analyzed using the FTDR Index [38]. The FTDR Index considers the summation of the difference between highest and lowest saturation degree of ice content in each complete or incomplete freeze-thaw cycle. A freeze-thaw cycle is defined as the process where the ice in the porous medium forms and then totally disappears. The calculation procedure for FTDR is:

$$FTDR\ Index = \sum_{cycle} (S_{\text{ice,max}} - S_{\text{ice,min}})\ \ when\ S_{\text{ice,max}} - S_{\text{ice,min}} > 0.05 \qquad (2)$$

A threshold difference value of 0.05 is introduced to disregard the influence of freeze-thaw cycles with very small variation of ice content. The FTDR Index considers both the effect of ice content difference over the freeze-thaw cycle and the number of freeze-thaw cycles. This index was found to be more realistic as the commonly used index in building physics is only based on the number of freeze-thaw cycles [38]. A higher value of FTDR Index indicates a higher risk of freeze-thaw damage. The critical FTDR Index for a specific porous material can be determined by performing freeze-thaw standard experiments.

3 Results

The final FTDR Index in the reference period 1980-2009 is 87.7 and 28.6 for Zurich and Davos, respectively (Figure 6). For Zurich, the final FTDR Indices range between 37.0 and 73.2 for the period 2021-2050 and between 19.8 and 47.7 for the period 2070-2099 (Figures 6 and 7). For Davos, the final FTDR Indices range between 35.8 and 71.2 for the period 2021-2050 and between 52.0 and 120.9 for the period 2070-2099 (Figures 6 and 7). Compared to final FTDR Index in the reference period 1980-2009, the final FTDR Indices for all future scenarios at Zurich decreases whereas they increase for all future scenarios at Davos.

3.1 Influence of emission scenarios

In general, the difference of FTDR Index between A1B and A2 scenarios is small (Figures 6 and 7). For example, the largest difference of final FTDR Index between the two scenarios is 11.4 for Davos in the period 2070-2099 with climate data from model chain ERM (Figure 7). This is much smaller than the difference caused by different model chains. Due to larger increase of temperature in A1B scenarios than A2 scenarios for the period 2021-2050 (Figure 5), there are generally larger changes of FTDR Indices for future climate scenarios associated with A1B scenario. By contrast, for the period 2070-2099 the increase of temperature is larger in A2 scenarios (Figure 5); there are slightly larger changes of FTDR Index for future climate scenarios associated with A2 scenarios.

3.2 Difference between reference period and future periods

For Zurich, climate change leads to smaller FTDR Indices compared to the reference period. The scenarios in the far future period 2070-2099 show smaller FTDR indices than the scenarios in the near future period 2021-2050. For Davos, it shows the completely reverse picture. Climate change result in larger FTDR Indices. The scenarios in the far future period 2070-2099 show larger FTDR Indices than the near future period 2021-2050.

For Zurich, air temperature in the cold period is mostly above 0 °C. An increase of air temperature that leads to less freeze-thaw cycles is the main reason for the lower risk of freeze-thaw damage in future at Zurich. Change of precipitation has very small influence on FTDR Index. In general, the model chains that have larger temperature increase in the cold period lead to larger decrease of FTDR Index (Table 1). For example, the model chains HH, HC and ERE that project largest temperature increase in the cold period show the smallest FTDR Indices in the period 2021-2050 and 2070-2099.

For Davos, air temperature in the cold period is mostly well below 0 °C. An increase of air temperature and precipitation is the reason for higher FTDR Indices. An increase of air

temperature will lead to more freeze-thaw cycles. When air temperature increase, more percentage of precipitation will occur in the form of rain. In addition, an increase of precipitation will lead to more rainfall and thus more wind-driven rain load on the wall surface. For Davos, in the period 2021-2050, the change of precipitation is relatively small and precipitation change has very small influence on increase of FTDR Indices. The model chains that have larger temperature increase have in general also larger FTDR Index (Table 2). In the period 2070-2099, the model chains that predict larger temperature increase project also larger precipitation increase. Consequently, the FTDR Indices under these model chains show significant FTDR Index increase. For example, the final FTDR Index with climate data from model chain HR reaches value up to 120.94 under A1B emission scenario. The precipitation and rainfall change from model chain HR under A1B scenario is shown in Figure 8 to clarify how temperature change affect rainfall at Davos. In the reference period 1980-2009, cold period precipitation is mainly in the form of snow at Davos. The amount of rainfall is relatively small. In the near future period 2021-2050, both precipitation and rainfall show small increase in the cold period compared to the reference period. In the far future period 2070-2099, the increase of rainfall is much larger than the increase of precipitation, which is mainly due to air temperature increase.

Zurich has a much higher risk of freeze-thaw damage than Davos in the reference period. The risk of freeze-thaw damage at Zurich is similar with Davos in near future period 2021-2050. However, the risk of freeze-thaw damage at Davos for the future period 2070-2099 becomes much higher than Zurich, illustrating a reversal of risks between the two locations.

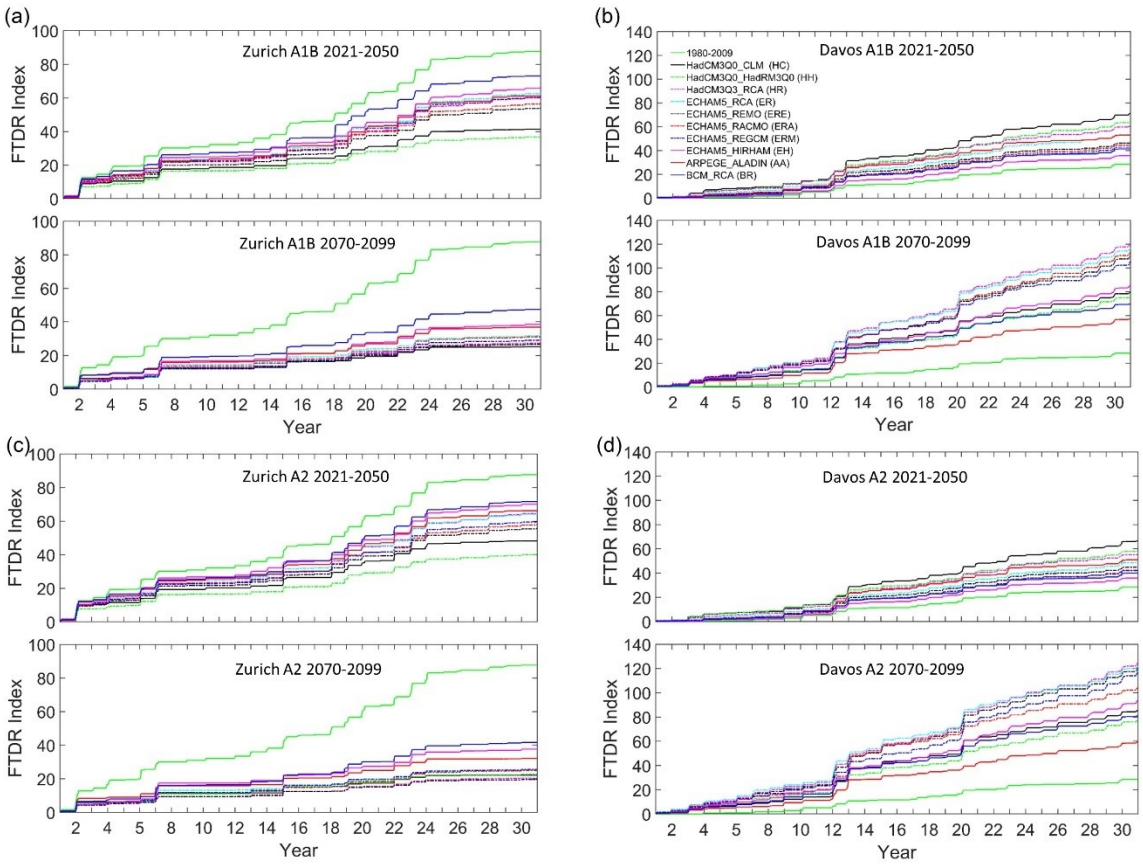

Figure 6. (a) FTDR Index for A1B climate scenarios for Zurich; (b) FTDR Index for A1B climate scenarios for Davos; (c) FTDR Index for A2 climate scenarios for Zurich; (d) FTDR Index for A2 climate scenarios for Davos. The green lines show the FTDR Index from the reference period.

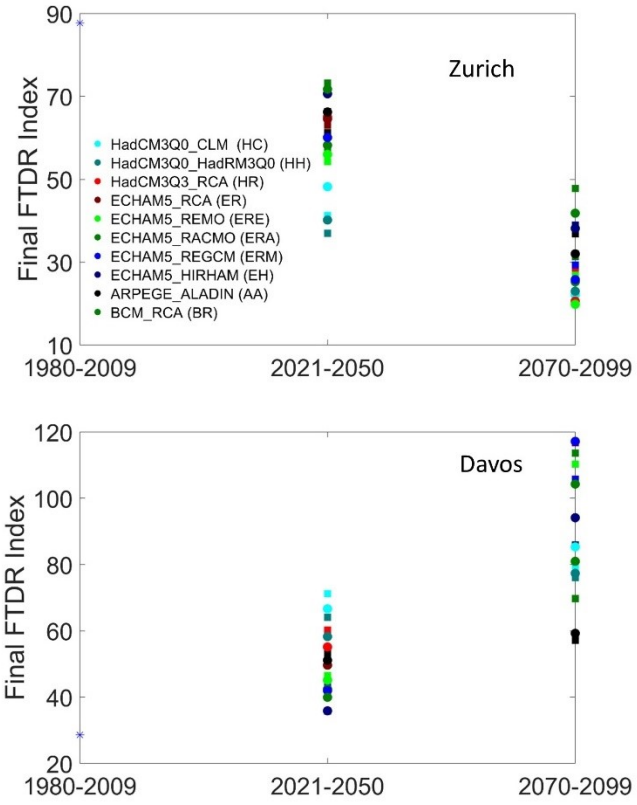

Figure 7. Final FTDR Index under different future projections at Zurich and Davos in the different periods. Scenarios are A1B (square) and A2 (Circle).

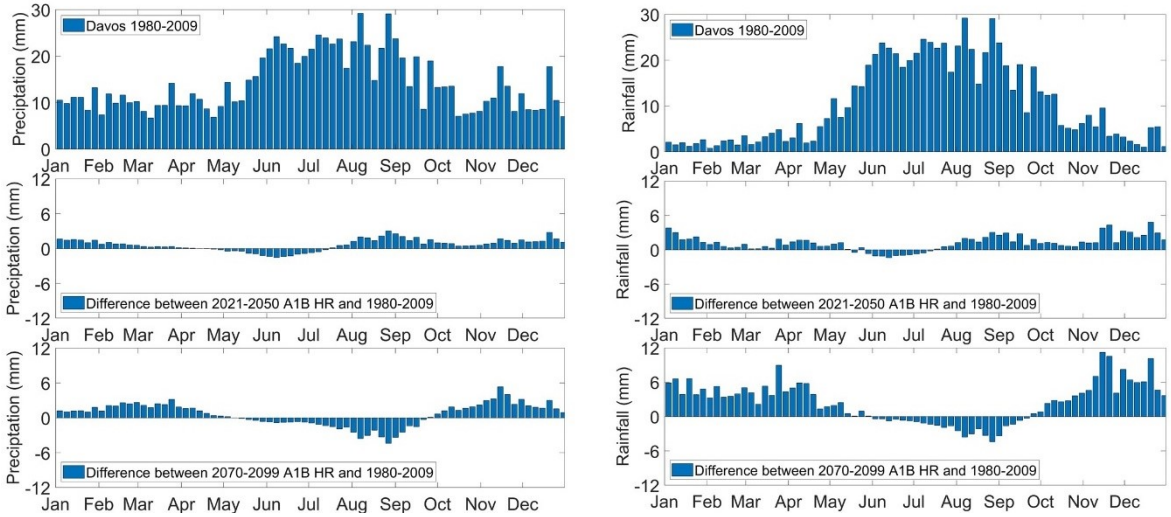

Figure 8. Mean values of five-day accumulated precipitation and rainfall at Davos over 30 years for climate model chain HR under A1B scenario, as well as the difference between the future period and the reference period.

3.3 Influence of climate model chains

In general, there is a large difference of FTDR Indices among the different climate model chains. For example, the final FTDR Indices under A1B emission scenario for the period 2070-2099 ranges between 25.2 and 47.75 at Zurich and between 57.2 and 120.9 at Davos (Figures 6 and 7). The range is much larger at Davos. For Zurich, the model chains that lead to higher FTDR Index in the near future period 2021-2050 also have higher FTDR Index in the far future period 2070-2099 (Table 1 and Figure 6). However, the ranking of final FTDR Index among model chains for Davos is very different between future periods 2021-2050 and 2070-2099. The ranking of temperature and precipitation change between the two periods at Davos is also very different (Table 2). For example, the final FTDR Index with model chain HC is the largest in the period 2021-2050 whereas it is only the sixth largest in the period 2070-2099. In 2070-2099, this model chain has large temperature increase of 3.27 K in the cold period. However, precipitation in the cold period decreases by 3 %. By comparison, most other model chains present an increase of precipitation. The decrease of precipitation is the main reason for small FTDR Index with this model chain in 2070-2099.

The ranking of final FTDR Index with model chain ERA is the 7th in 2021-2050. However, the ranking of final FTDR Index of this model chain is the 3rd in the period 2070-2099. It presents considerably large temperature and precipitation increase in the period 2070-2099 whereas the temperature and precipitation increase is relatively small in the period 2021-2050. Figure 9 shows the influence temperature and precipitation change on ice content and thus FTDR Index in detail. Due to diurnal change of temperature, freezing occurs during the night and thawing occurs during the day. The reference period has the lowest total moisture content. Although this period has the lowest temperature, there is not so much amount of water available for freezing. The ice content stays at low level. The model chain ERA in the period 2070-2099 has the largest total moisture content due to large precipitation increase. When freezing occurs, a sufficient amount of water is available for freezing. Therefore, this scenario has very high ice content. Although the model chain HH has larger temperature increase compared to the model chian ERA, this model chain presents lower ice content as it has smaller precipitation increase and thus lower total moisture content.

Table 1. Final FTDR Index, change in mean temperature and precipitation from November to March for Zurich under A1B emission scenario.

Zurich 2021-2050				Zurich 2070-2099			
Model chain	Final FTDR Index	ΔT (K)	ΔP (%)	Model chain	Final FTDR Index	ΔT (K)	ΔP (%)
HH	36.99	1.57	2.90	HC	25.20	3.23	-1.19
HC	41.25	1.62	-1.96	HH	26.85	3.19	13.53
ERE	54.23	1.10	1.70	ERE	26.87	3.02	16.31
ERA	56.83	1.04	6.29	HR	27.64	2.99	21.82
HR	60.71	1.11	18.56	ERM	29.31	2.77	15.83
ERM	60.83	0.87	1.44	ERA	31.39	3.07	25.52
AA	61.19	0.89	-0.45	ER	31.99	2.82	25.37
ER	63.03	0.98	8.91	AA	36.84	1.94	-4.10
EH	66.34	0.74	5.40	EH	38.92	2.45	24.37
BR	73.19	0.85	8.97	BR	47.75	1.97	15.96

Table 2. Final FTDR Index, change in mean temperature and precipitation from November to March for Davos under A1B emission scenario.

Davos 2021-2050				Davos 2070-2099			
Model chain	FTDR Index	ΔT (K)	ΔP (%)	Model chain	FTDR Index	ΔT (K)	ΔP (%)
HC	71.18	1.56	3.61	HR	120.94	3.51	20.90
HH	64.10	1.67	0.78	ER	116.74	3.42	15.27
HR	60.19	1.08	9.87	ERA	113.59	2.99	17.12
ER	54.09	1.12	2.20	ERE	110.29	3.31	12.81
AA	53.11	1.18	-4.45	ERM	105.75	2.77	14.83
ERE	46.49	1.04	1.40	EH	85.89	2.41	12.14
ERA	44.63	0.97	2.64	HC	79.22	3.27	-3.00
ERM	42.88	0.79	1.52	HH	76.11	3.54	-2.91
BR	41.31	0.71	1.33	BR	69.75	2.00	0.32
EH	35.81	0.66	1.79	AA	57.19	2.47	-12.12

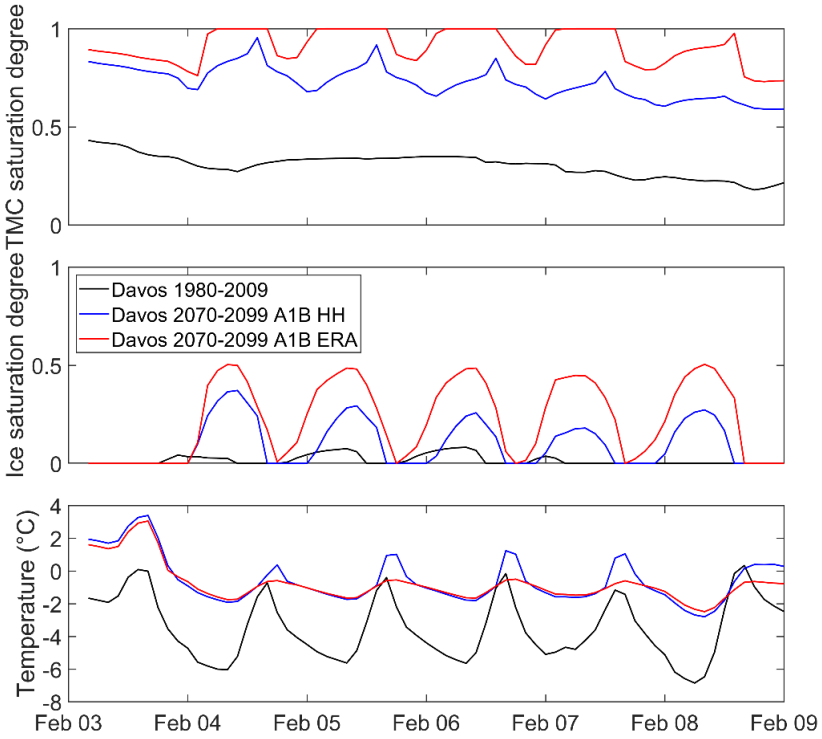

Figure 9. Total moisture content saturation degree, ice content saturation degree and temperature from February 3 to February 9 at the 12th year under A2 scenario in reference and future periods at Davos.

4 Discussion and conclusion

The impact of climate change on risk of freeze-thaw damage for internally insulated masonry wall in two regions of Switzerland with very different climates for the reference period 1980-2009, the near future period 2021-2050 and far future period 2070-2099 is evaluated in this study. A hygrothermal model tracking the occurrence of freezing and thawing is used to simulate hygrothermal condition in the internally insulated masonry wall. The risk of freeze-thaw damage in the masonry wall is evaluated with the FTDR Index. The IPCC A1B and A2 emission scenarios and ten different climate model chains have been chosen to cover a larger range of future climate conditions. An increase of air temperature that leads to less freeze-thaw cycles is the main reason for the lower risk of freeze-thaw damage in the future periods at Zurich. By comparison, the increase of temperature and precipitation in the cold period is the main reason for higher risk of freeze-thaw damage in the future periods at Davos. The difference caused by different emission scenarios is much smaller than that caused by different climate model chains. Climate change impact studies based on results from single or limited model chains should be interpreted with caution.

Utilization of projections from an ensemble of different climate models under different emission scenarios is possible better to cover the uncertainty associated with climate projections. Quantifying the uncertainties in projections of climate change and its impacts is essential for helping policy-makers in implementing adaptation plans and mitigation measures. The uncertainty of FTDR Index at Davos in period 2070-2099 is much larger than that of Zurich. The uncertainty of FTDR Index is mainly correlated to the uncertainty of projections for temperature at Zurich whereas the uncertainty of FTDR Index is correlated to the uncertainty of projections for temperature and precipitation at Davos. In the period 2021-2050 at Davos, temperature change is between 0.66 and 1.67 K and precipitation change is between -4.45 and 9.87 % in the cold period. By comparison, in the period 2070-2099, temperature change is between 2.00 and 4.17 K and precipitation change is between -14.27 and 23.44 % in the cold period. The larger uncertainty of projections for temperature and precipitation in the period 2070-2099 leads to larger uncertainty of FTDR Index at Davos compared to the period 2021-2050.

Even though the future climate has some uncertainties, the general trend with respect to risk of freeze-thaw damage seems to show clear trends. For Zurich, the risk of freeze-thaw damage is relatively high in the reference period. The risk of freeze-thaw damage in the future in Zurich will be much smaller than the current period. Climate change tends to reduce damage caused by freeze-thaw cycles at this location. However, for Davos, the current risk of freeze-thaw damage is quite low. There will be much higher risk of freeze-thaw damage under future climate conditions. The current requirement on measures against freeze-thaw damage is possibly relatively low at Davos. In the face of climate change, the future requirement on frost resistance of building materials and components at Davos should take the future climate loading into account. Although the focus of the study is on Switzerland, it is possible to extend the analysis to other parts of world. The findings from this study also apply to the impact of climate change on freeze-thaw damage for other porous building materials that are exposed to climatic loadings in these two regions.

Emission scenarios is a crucial part of climate change study and assessment. They enable us to examine different possible futures in the context of future uncertainties. A limitation of this study is that the used A1B and A2 emission scenarios do not explicitly include the effect of climate change policies on carbon emissions controls. The newer scenarios, called Representative Concentration Pathways (RCPs) from IPCC 5th Assessment Report [46], can consider climate change mitigation policies to limit emissions. They are consistent with a wide range of possible changes in future anthropogenic emissions, and aim to represent their atmospheric concentrations. The latest scenarios, Sharing Socioeconomic Paths Scenario (SSPs) [47], depict the future socio-economic developments and the climate change mitigation and adaptation challenges they face through key elements such as

population, economic growth, education, lifestyle, urbanization, environment and natural resources, policies and institutions [48]. They reflect the combined effects of climatic factors and socio-economic factors, satisfying the needs of different research fields such as climate change impact, adaptation and mitigation.

Acknowledgement

The CH2011 data were obtained from the Center for Climate Systems Modeling (C2SM). This research project is part of the Swiss Competence Center for Energy Research SCCER FEEB&D of the Swiss Innovation Agency Innosuisse.

References

[1] R.K. Pachauri, A. Reisinger, IPCC fourth assessment report, IPCC, Geneva. 2007 (2007).

[2] N. Nakicenovic, J. Alcamo, A. Grubler, K. Riahi, R.A. Roehrl, H.-H. Rogner, N. Victor, Special report on emissions scenarios (SRES), a special report of Working Group III of the intergovernmental panel on climate change, Cambridge University Press, 2000.

[3] Meteoswiss, Climate Change in Switzerland, (2019). https://www.meteoswiss.admin.ch/home/climate/climate-change-in-switzerland.html.

[4] A.G. Prognos, Erläuternder Bericht Zur Energiestrategie 2050, Switz. Bundesamt Für Energie. Www. Energiestrategie2050. Ch. (2013).

[5] P. De Wilde, D. Coley, The implications of a changing climate for buildings, (2012).

[6] V.M. Nik, A.S. Kalagasidis, Impact study of the climate change on the energy performance of the building stock in Stockholm considering four climate uncertainties, Build. Environ. 60 (2013) 291–304.

[7] M.A. Lacasse, An overview of durability and climate change of building components, Can. J. Civ. Eng. 46 (2019) v–viii.

[8] M.C. Phillipson, R. Emmanuel, P.H. Baker, The durability of building materials under a changing climate, Wiley Interdiscip. Rev. Clim. Chang. 7 (2016) 590–599.

[9] V.M. Nik, A.S. Kalagasidis, E. Kjellström, Assessment of hygrothermal performance and mould growth risk in ventilated attics in respect to possible

climate changes in Sweden, Build. Environ. 55 (2012) 96–109.

[10] V.M. Nik, S.O. Mundt-Petersen, A.S. Kalagasidis, P. De Wilde, Future moisture loads for building facades in Sweden: Climate change and wind-driven rain, Build. Environ. 93 (2015) 362–375.

[11] V.M. Nik, Climate Simulation of an Attic Using Future Weather Data Sets-Statistical Methods for Data Processing and Analysis, (2010).

[12] V.M. Nik, Application of typical and extreme weather data sets in the hygrothermal simulation of building components for future climate–A case study for a wooden frame wall, Energy Build. 154 (2017) 30–45.

[13] C. Sabbioni, P. Brimblecombe, M. Cassar, The atlas of climate change impact on European cultural heritage: scientific analysis and management strategies, Anthem Press, 2010.

[14] A. Köliö, T.A. Pakkala, J. Lahdensivu, M. Kiviste, Durability demands related to carbonation induced corrosion for Finnish concrete buildings in changing climate, Eng. Struct. 62 (2014) 42–52.

[15] Z. Huijbregts, R.P. Kramer, M.H.J. Martens, A.W.M. Van Schijndel, H.L. Schellen, A proposed method to assess the damage risk of future climate change to museum objects in historic buildings, Build. Environ. 55 (2012) 43–56.

[16] V. Nik, Mould Growth inside an Attic concerning Four Different Future Climate Scenarios, in: 9th Nord. Symp. Build. Physics-NSB 2011, 2011: pp. 841–848.

[17] V.M. Nik, Hygrothermal simulations of buildings concerning uncertainties of the future climate, Chalmers University of Technology, 2012.

[18] A. Sehizadeh, H. Ge, Impact of future climates on the durability of typical residential wall assemblies retrofitted to the PassiveHaus for the Eastern Canada region, Build. Environ. 97 (2016) 111–125.

[19] K. Hall, Evidence for freeze–thaw events and their implications for rock weathering in northern Canada, Earth Surf. Process. Landforms J. Br. Geomorphol. Res. Gr. 29 (2004) 43–57.

[20] C.M. Grossi, P. Brimblecombe, I. Harris, Predicting long term freeze–thaw risks on Europe built heritage and archaeological sites in a changing climate, Sci. Total Environ. 377 (2007) 273–281.

[21] I. Vandemeulebroucke, K. Calle, S. Caluwaerts, T. De Kock, N. Van Den Bossche, Does historic construction suffer or benefit from the urban heat island effect in Ghent and global warming across Europe?, Can. J. Civ. Eng. 46 (2019) 1032–1042.

[22] H.A. Viles, Implications of future climate change for stone deterioration, Geol. Soc.

London, Spec. Publ. 205 (2002) 407–418.

[23] P. Brimblecombe, D. Camuffo, Long term damage to the built environment, Eff. Air Pollut. Built Environ. 2 (2003) 1–30.

[24] T.A. Pakkala, A. Köliö, J. Lahdensivu, M. Kiviste, Durability demands related to frost attack for Finnish concrete buildings in changing climate, Build. Environ. 82 (2014) 27–41.

[25] G.W. Scherer, Crystallization in pores, Cem. Concr. Res. 29 (1999) 1347–1358.

[26] O. Coussy, P. Monteiro, Unsaturated poroelasticity for crystallization in pores, Comput. Geotech. 34 (2007) 279–290.

[27] D.H. Everett, The thermodynamics of frost damage to porous solids, Trans. Faraday Soc. 57 (1961) 1541–1551.

[28] G. Fagerlund, Determination of pore-size distribution from freezing-point depression, Matériaux Constr. 6 (1973) 215–225.

[29] C. Maclnnis, J.J. Becaudoin, Effect of degree of saturation on the frost resistance of mortar mixes, in: J. Proc., 1968: pp. 203–208.

[30] M.C. Phillipson, A.W. Stupart, Determination of the freezing point of water in a porous masonry material, Mason. Int. 12 (1998) 17–20.

[31] J. Straube, C. Schumacher, P. Mensinga, Assessing the freeze-thaw resistance of clay brick for interior insulation retrofit projects, in: Proc., Build. XI Conf., ASHRAE (American Soc. Heating, Refrig. Air-Conditioning Eng. Clear. FL, 2010.

[32] X. Zhou, D. Derome, J. Carmeliet, Robust moisture reference year methodology for hygrothermal simulations, Build. Environ. 110 (2016) 23–35. doi:10.1016/j.buildenv.2016.09.021.

[33] E. Vereecken, S. Roels, Capillary active interior insulation: do the advantages really offset potential disadvantages?, Mater. Struct. 48 (2015) 3009–3021.

[34] M. Guizzardi, J. Carmeliet, D. Derome, Risk analysis of biodeterioration of wooden beams embedded in internally insulated masonry walls, Constr. Build. Mater. 99 (2015) 159–168. doi:10.1016/j.conbuildmat.2015.08.022.

[35] X. Zhou, J. Carmeliet, D. Derome, Influence of envelope properties on interior insulation solutions for masonry walls, Build. Environ. 135 (2018) 246–256. doi:10.1016/j.buildenv.2018.02.047.

[36] A.H.P. Maurenbrecher, C.J. Shirtliffe, M.Z. Rousseau, M.N.A. Saïd, Monitoring the hygrothermal performance of a masonry wall with and without thermal insulation, in: Proc. 8th Can. Mason. Symp., Citeseer, 1998: pp. 174–193.

[37] H.M. Künzel, Effect of interior and exterior insulation on the hygrothermal behaviour of exposed walls, Mater. Struct. 31 (1998) 99–103.

[38] X. Zhou, D. Derome, J. Carmeliet, Hygrothermal modeling and evaluation of freeze-thaw damage risk of masonry walls retrofitted with internal insulation, Build. Environ. 125 (2017) 285–298. doi:10.1016/j.buildenv.2017.08.001.

[39] C. Appenzeller, I. Bey, M. Croci Maspoli, J. Fuhrer, R. Knutti, C. Kull, C. Schär, Swiss climate change scenarios CH2011, ETH Zurich, 2011.

[40] G. Flato, J. Marotzke, B. Abiodun, P. Braconnot, S.C. Chou, W. Collins, P. Cox, F. Driouech, S. Emori, V. Eyring, Evaluation of climate models, in: Clim. Chang. 2013 Phys. Sci. Basis. Contrib. Work. Gr. I to Fifth Assess. Rep. Intergov. Panel Clim. Chang., Cambridge University Press, 2014: pp. 741–866.

[41] M. Guizzardi, Hygrothermal performance assessment of novel interior insulation solutions, (2014).

[42] H. Janssen, B. Blocken, J. Carmeliet, Conservative modelling of the moisture and heat transfer in building components under atmospheric excitation, Int. J. Heat Mass Transf. 50 (2007) 1128–1140. doi:10.1016/j.ijheatmasstransfer.2006.06.048.

[43] T. Bosshard, S. Kotlarski, C. Schär, Local scenarios at daily resolution for emission scenarios A2 and RCP3PD, CH2011 Ext. Ser. No. 1. (2011).

[44] A. TenWolde, ASHRAE Standard 160P--criteria for moisture control design analysis in buildings, (2008).

[45] X. Zhou, J. Zhou, W. Kinzelbach, F. Stauffer, Simultaneous measurement of unfrozen water content and ice content in frozen soil using gamma ray attenuation and TDR, Water Resour. Res. 50 (2014) 9630–9655.

[46] R.K. Pachauri, M.R. Allen, V.R. Barros, J. Broome, W. Cramer, R. Christ, J.A. Church, L. Clarke, Q. Dahe, P. Dasgupta, Climate change 2014: synthesis report. Contribution of Working Groups I, II and III to the fifth assessment report of the Intergovernmental Panel on Climate Change, Ipcc, 2014.

[47] B.C. O'Neill, E. Kriegler, K. Riahi, K.L. Ebi, S. Hallegatte, T.R. Carter, R. Mathur, D.P. van Vuuren, A new scenario framework for climate change research: the concept of shared socioeconomic pathways, Clim. Change. 122 (2014) 387–400.

[48] L. Jiang, B.C. O'Neill, Global urbanization projections for the Shared Socioeconomic Pathways, Glob. Environ. Chang. 42 (2017) 193–199.